PAPER Nr.: 101



APPLICATION OF THE WIDE-FIELD SHADOWGRAPH TECHNIQUE TO ROTOR WAKE VISUALIZATION

BY

THOMAS R. NORMAN AND JEFFREY S. LIGHT
NASA AMES RESEARCH CENTER
MOFFETT FIELD, CALIFORNIA

FIFTEENTH EUROPEAN ROTORCRAFT FORUM

SEPTEMBER 12 - 15, 1989 AMSTERDAM

APPLICATION OF THE WIDE-FIELD SHADOWGRAPH TECHNIQUE TO ROTOR WAKE VISUALIZATION

by

Thomas R. Norman and Jeffrey S. Light
NASA Ames Research Center
Moffett Field, California

Abstract

This paper reviews the wide-field shadowgraph technique and its application to the visualization of rotor wakes. In particular, it discusses current experimental methods and data-reduction requirements. Sample shadowgraphs are presented. These include shadowgraphs of model-scale helicopter main rotors and tilt rotors, and full-scale tail rotors, both in hover and in forward flight.

Notation

C_T = rotor thrust coefficient
h = rotor distance from ground plane, m
M_t = tip Mach number
R = rotor radius, m
r = radial distance, m
z = axial distance, m
μ = advance ratio
σ = rotor solidity

1. Introduction

The ability to accurately measure the tip vortex geometry of rotors in hover and forward flight has been and will continue to be extremely valuable. For example, instantaneous vortex trajectories have helped to provide physical insight into the flow phenomena causing rotor wake distortion (Ref. 1). Averaged tip vortex coordinates have helped in the development of empirical prescribed-wake models used to predict rotor hover performance (Refs. 1,2). In addition, both the instantaneous and the averaged wake data have been used to validate new rotor wake models, such as those found in free-wake analyses (Ref. 3).

A number of flow-visualization methods have been used to provide qualitative and/or quantitative information about the tip vortex geometry of rotor systems. One relatively simple method involves injecting smoke at or near the rotor-blade tip (Ref. 1). This method provides the ability to measure tip vortex geometry coordinates at a single location. Unfortunately, smoke diffusion and the intrusive nature of the smoke injection hardware can limit the method's usefulness. Another flow-visualization method uses the schlieren technique (Ref. 1,2) to visualize the entire tip vortex trajectory. Although the results using this method are quite good, the optical complexity and the required alignment precision make this method difficult to implement and practical only for very small model rotors.

A third method with which rotor tip vortices can be visualized is the wide-field shadowgraph technique (Refs. 4,5). This technique provides tip vortex trajectories comparable in detail to the schlieren method, but without the optical complexity. In addition, the

shadowgraph technique does not have any fundamental limitation on the size of the viewing area; thus wakes can be visualized for rotors ranging from model- to full-scale.

The objective of this paper is to review this wide-field shadowgraph technique as it applies to rotor wake visualization. In particular, the capabilities and limitations of both the experimental technique and data-reduction method are discussed. In addition, a summary of recently completed shadowgraph experiments is presented, including sample shadowgraphs and samples of reduced data.

2. Experimental Technique

2.1 Test Setup

In order to visualize rotor tip vortices with the wide-field shadowgraph technique, the following components are required: 1) an imaging device (still or video camera); 2) a short-duration, high-intensity, point-source light (usually a strobe); and 3) a retroreflective screen. An example of how these components may be configured is shown in Figure 1. With this setup, light passes through the rotor wake, casting shadows on the screen. These shadows are the result of changes in the refractive index of the air caused by naturally occurring density gradients in the tip vortex cores (Ref. 6). A permanent record of these shadow patterns can then be acquired with an imaging device focused on the retroreflective screen. The tip vortices are visible as thin dark spirals emanating from the rotor blade tips.

Figure 1 shows one possible experimental arrangement, with shadowgraphs acquired from the side of the rotor. With the strobe, camera, and screen at the approximate rotor-plane height, this setup allows both radial and axial tip vortex coordinates to be determined. Figure 2 shows an alternate arrangement, with shadowgraphs acquired from above the rotor. This setup provides a good method for looking at wake contraction or determining the location of blade/vortex interaction.

2.2 Data Acquisition

The majority of shadowgraph data acquired to date has been with a still camera as the imaging device. Shadowgraphs are acquired by opening the camera shutter and electronically triggering the light source to fire at a specified rotor azimuth position. For a given rotor condition (thrust, tip Mach number, etc.), shadowgraphs are acquired over a range of azimuth positions, with at least three or four acquired at each azimuth. This is necessary to map out the average radial and axial movements of the tip vortices as a function of wake age.

With the use of a still camera, high-quality, high-resolution shadowgraphs can be acquired. There are a number of drawbacks to this method, however. The biggest problem is the lack of real-time feedback on the shadowgraphs. Problems with the camera, the experimental setup, or the run conditions cannot be detected until the film is developed, well after the run is completed. This may cause significant delays in the test schedule, with entire runs needing to be repeated.

In order to address these concerns, NASA has begun using a video camera as the imaging device. The use of video has a number of advantages: 1) immediate feedback on shadowgraphs (can find setup errors and determine best conditions), 2) very fast data acquisition (every frame is one shadowgraph), and 3) highly flexible test setup (camera can be panned, tilted, or zoomed to focus on area of interest). The major drawback to this technique

is the lower resolution associated with video. Work is currently under way to determine the severity of this problem.

Depending on the research objectives, additional data are normally required to complement the shadowgraph data. This additional data may be divided into two categories: 1) data required for reducing the shadowgraphs (such as test setup geometry), and 2) data required for correlating the shadowgraph data with predictions. Examples of the second category include tip Mach Number, thrust coefficient, power coefficient, advance ratio, and blade azimuth position.

3. Shadowgraph Tests Conducted

Several tests have been conducted to develop the wide-field shadowgraph method for use in visualizing rotorcraft tip vortices (summarized in Table 1). These tests have covered many helicopter flight regimes including hover, hover in-ground-effect, and forward flight. A short summary of each of these tests is presented below, with more complete descriptions available in the references.

Initial shadowgraph development work was performed by the Jet Propulsion Laboratory under a NASA contract (Ref. 4). This effort was the first to apply the shadowgraph process to the visualization of rotor tip vortices. The rotor system used for this work was a Hughes Model 300 tail rotor (characteristics supplied in Table 2). A sample of the shadowgraphs obtained in this test is shown in Figure 3. Tip vortex trajectories are visible in this figure as thin spirals above the rotor. The main objective of this work was to examine the effect of test setup (camera-to-rotor and rotor-to-screen distances) and rotor operating parameters on the visibility of the tip vortices. Of note in Figure 3 (and all subsequent shadowgraphs) are the "double images" of the rotor blades and test hardware. These are caused by the camera and light source being separated by a finite distance. The resultant shadowgraphs thus contain both the image of an object and the image of the object's shadow. Note that since the camera is focused on the screen, the shadows are the sharper of these images.

The first test conducted by NASA to further develop the shadowgraph method was a hover test of a 0.16-scale model of the Sikorsky S-76 rotor (Ref. 5). The blades were dynamically and geometrically similar to S-76 blades, except the model blades had rectangular tips instead of swept-tapered tips (Table 2). The rotor system was tested in two configurations. The first was a conventional thrust-up, wake-down configuration with the rotor plane located 5.71 rotor radii above the ground. In order to eliminate any test stand or ground interference, a second configuration was tested. This was a thrust-down, wake-up configuration with the rotor plane located 2.86 rotor radii above the ground. A sample shadowgraph from the wake-down configuration is shown in Figure 4. The contraction of the wake and the descent of subsequent turns of wake are clearly evident in this photo. This test demonstrated the ability of the shadowgraph technique to provide the necessary data to define the geometry of the tip vortices of a hovering rotor.

The second shadowgraph test performed by NASA (with U.S. Army cooperation) was of a model tilt rotor in hover. This model, tested in the settling chamber of the Ames Research Center 7- by 10-Foot Wind Tunnel, consisted of a rotor, a nacelle, and a wing spar. The characteristics of this rotor are summarized in Table 2. The shadowgraphs acquired during this program provided very high-quality photos of the tip vortex geometry. Up to four blade passages were visible in some photos (Fig. 5). Other important phenomena found in these shadowgraphs included instabilities in the rotor wake and interactions between the tip vortex and the wing spar. Results from this test are also documented in Reference 5.

The next major shadowgraph test program was performed with a full-scale Lynx tail rotor. Characteristics of this rotor are provided in Table 2. The main objective of this program was to examine the effect of a ground plane on the tip vortex geometry of a hovering helicopter rotor (Ref. 7). To accomplish this, a circular ground plane (6.62 rotor radii in diameter) was mounted in the outflow of the Lynx tail rotor. The distance between the ground plane and the rotor was varied by moving the rotor toward or away from the ground plane. Shadowgraphs were acquired at a number of rotor conditions and rotor/ground plane separations. Figure 6 is an example of one such shadowgraph at a small separation distance. Significant expansion of the rotor wake and a decrease in the tip vortex descent rate are visible in this figure. During this test, very high-quality shadowgraphs were obtained, with some photos showing up to five blade passages (Fig. 7).

The applicability of the wide-field shadowgraph method to forward flight was first examined during a joint Army/NASA/Boeing test program at the Duits Nederlandse Windtunnel (DNW) using a 1/5-scale Boeing Model 360 rotor. General characteristics of this rotor are provided in Table 2 with additional information available in Reference 8. Shadowgraphs were acquired from below the advancing side of the rotor (Fig. 8) with a test configuration similar to that shown in Figure 2. At low advance ratios ($\mu < 0.08$) the vortices were clearly visible as they were swept behind the rotor (Fig. 9). At higher forward speeds, the tip vortices were not visible. The cause of this loss of visibility has not yet been determined.

A second wind tunnel test was recently conducted by NASA Ames researchers to examine tip vortex geometry in forward flight. This test was conducted at the University of Maryland's Glenn L. Martin Wind Tunnel using a small-scale four-bladed rotor. During this test, shadowgraphs were acquired both from above and from the side of the rotor system for a wide range of operating conditions in forward flight (up to $\mu = 0.175$). In particular, separate shadowgraphs were acquired showing the front and rear portions of the rotor system. Figure 10 is a sample shadowgraph showing the front half of the rotor system at a low forward speed (air flow from right to left). This shadowgraph provides information on tip vortex trajectories in forward flight and blade/vortex interactions (see second blade passage). Figure 11 is a sample showing the rear half of the rotor system. This shadowgraph also provides information on the tip vortex trajectories and on wake/fuselage interactions in forward flight. In addition to still-photo shadowgraphs such as these, this test also provided the first known videos of tip vortices using the wide-field shadowgraph technique.

4. Limitations of Experimental Technique

Despite its excellent capabilities, the wide-field shadowgraph technique does have some limitations. In particular, the tip vortex strength plays a major role in whether the vortices are visible. Previous work attempting to quantify the vortex visibility (Ref. 5) demonstrated that a minimum strength is necessary for adequate visibility. For those rotor systems tested so far, this corresponds to full-scale tip Mach numbers ($M_t > 0.5$) and moderate thrust values ($C_T/\sigma > 0.06$).

It has also been noted that vortex visibility is greatly reduced when the rotor blades reach stall. At this condition, the strength of the tip vortices decreases significantly. Thus, the shadowgraph technique is applicable to a limited envelope of operating conditions. Fortunately, a significant amount of interesting flight conditions are included in this envelope.

Forward flight is another condition which affects tip vortex strength and thus vortex visibility. A simple analysis (Ref. 5) suggests that vortex visibility should decrease with forward speed on the advancing side of the rotor and increase on the retreating side (caused by

changes in blade angle of attack around the azimuth in forward flight). Preliminary results seem to indicate that the vortex visibility decreases on both sides of the rotor. Additional work must be performed to understand this effect.

5. Data-Reduction Method

Shadowgraph data-reduction methods are necessary in order to provide quantitative information about rotor tip vortex trajectories. In general, separate methods are required for each test configuration. For example, different methods are required if shadowgraphs are acquired from the top rather than from the side of the rotor. Also, different methods are required for reducing hover and forward flight data.

Currently, NASA has a complete data-reduction method for only one test configuration: shadowgraphs acquired from the side of a hovering rotor. A review of this method is provided in the following section, followed by sample results and future data-reduction plans.

5.1 Current Method – Hover

The current data-reduction method reduces shadowgraphs acquired from the side view of a hovering rotor to provide axial and radial tip vortex coordinates as a function of wake azimuth angle. The primary assumptions of the method are 1) the tip vortex trajectories are nominally helical in nature, and 2) the trajectories are centered about the rotor centerline.

For the data reduction method to be successful, each shadowgraph must provide certain basic information. First, all blade tips must be visible on the shadowgraph. The blade tips are used in conjunction with the known blade azimuth angles to define the tip path plane of the rotor. Second, the rotor centerline must be visible in the shadowgraph. The tip path plane and the rotor centerline are used as the baseline axes in the data processing. Lastly, two points on the screen at a known distance apart must be visible on the shadowgraph. These are used to scale the shadowgraph measurements to full-scale values.

Once this basic information has been provided, the tip vortex coordinates from a particular shadowgraph can be determined. The current method uses only the outermost points of the tip vortex trajectories in the data-reduction process. Measurements are made between these vortex points and the baseline axes (tip path plane and rotor centerline) projected on the shadowgraph screen. These measurements are then converted, based on the geometry of the test setup, to actual distances at the rotor. From these distances, radial and axial tip vortex coordinates are then easily determined.

This data-reduction method is currently operational on a DEC VAX computer using an x-y graphics tablet as the data input device. Inaccuracies of the calculated tip vortex coordinates are estimated to be approximately 1-1.5% of the rotor radius. This error can be mainly attributed to the method with which the tip path plane and rotor centerline are determined. Repeatability of the calculated tip vortex coordinates from one shadowgraph to the next has generally been within 1% of the rotor radius for points in the near wake. In the far wake, however, wake unsteadiness becomes apparent, with fluctuations ranging up to 15% of the radius.

5.2 Sample Results

Typical results generated by this method are shown in Figures 12 and 13. These figures plot the axial and radial tip vortex coordinates for one operating condition

($C_T/\sigma = 0.091$, out of ground effect) from the Lynx tail rotor test (Ref. 7). The data plotted here required data reduction of 40 different shadowgraph photos. Also plotted on these figures are theoretical and empirical predictions of the vortex coordinates. This demonstrates how shadowgraph data may be used to validate performance analyses (and their assumptions). The unsteadiness in the far wake is also visible in these figures, seen as data scatter at the high wake angles. The shadowgraph method provides one means of quantifying this unsteadiness.

Reference 7 demonstrated how this data-reduction method could be used to study the effects of rotor/ground separation on tip vortex geometry. Data were reduced for a number of rotor conditions and rotor/ground separation distances. Figure 14 is an example of reduced data at a small separation distance ($h/R = 0.32$); this shows the effect of the ground plane on the radial tip vortex coordinate. Figure 15 demonstrates how, by combining data from several conditions, the data reduction method can be utilized to quantify the effect of separation distance on tip vortex geometry.

Figure 16 demonstrates how this method might be used to study rotor wake interactions with solid bodies (i.e., wake/wing, wake/fuselage interaction). These data were acquired with the model tilt rotor configuration of Reference 5 (Table 2, Fig. 5). For this particular experiment, the shadowgraph light source was positioned so that all tip vortex geometry data from the right side of the rotor was acquired directly over the wingspan. Thus, the difference in tip vortex geometry between the right and left sides of the rotor is caused by the interference from the wingspan.

5.3 Future Plans

Although the current data-reduction method is capable of providing valuable information, more work needs to be done. Currently, work is under way to generalize and document the existing method. Also, since the use of video seems so promising, future plans include applying this method to video-acquired shadowgraphs. Work may need to be done to speed up the data-reduction process (image processing) in order to handle the larger amount of data available with the video.

The next step will be to develop data-reduction methods for forward flight. Separate methods will be required, depending on the phenomena of interest: wake geometry, wake/body interaction, blade/vortex interaction. It is expected that the current hover method will be adaptable to measuring wake geometry in forward flight.

6. Concluding Remarks

Through a number of recently conducted experiments, it has been shown that the wide-field shadowgraph technique is an excellent method for visualizing rotor wakes. For hovering rotors, in particular, detailed shadowgraphs showing complete tip vortex trajectories are possible. Quantitative data, in the form of tip vortex coordinates, can be determined using existing data-reduction methods.

The shadowgraph technique has also been shown to apply to low-speed forward flight. Quantitative data can be acquired, which detail tip vortex geometry in forward flight, including wake/fuselage and blade/vortex interactions. At this time, it is unclear whether high-speed forward flight data can be acquired. Additional testing is required to quantify the effect of forward speed on vortex visibility.

7. References

1) A. J. Landgrebe, The Wake Geometry of a Hovering Helicopter Rotor and its Influence on Rotor Performance, Journal of the American Helicopter Society, Vol. 17, (4), Oct. 1972.
2) J. D. Kocurek, and J. L. Tangler, , A Prescribed Wake Lifting Surface Hover Performance Analysis, American Helicopter Society 32nd Annual National Forum, Washington, DC, May 1976.
3) F. F. Felker, T. R. Quackenbush, D. B. Bliss, and J. S. Light, Comparisons of Predicted and Measured Rotor Performance in Hover Using a New Free Wake Analysis, American Helicopter Society 44th Annual National Forum, Washington, DC, June 1988.
4) S. P. Parthasarathy, Y. I. Cho, and L. H. Back, Wide-Field Shadowgraph Flow Visualization of Tip Vortices Generated by a Helicopter Rotor, AIAA Paper 85-1557, 18th AIAA Fluid Dynamics and Plasmadynamics and Lasers Conference, Cincinnati, Ohio, July 1985.
5) T. R. Norman, and J. S. Light, Rotor Tip Vortex Geometry Measurements Using the Wide-Field Shadowgraph Technique, Journal of the American Helicopter Society, April, 1987.
6) W. Merzkirch, Flow Visualization, Academic Press, Inc., NY, 1974, pp. 76-86.
7) J. S. Light, Tip Vortex Geometry of a Hovering Helicopter Rotor in Ground Effect, American Helicopter Society 45th Annual National Forum, Boston, Massachusetts, May 1989.
8) L. Dadone, S. Dawson, D. Boxwell, and D. Ekquist, Model 360 Rotor Test at DNW—Review of Performance and Blade Airload Data, American Helicopter Society 43rd Annual National Forum, St. Louis, Missouri, May 1987.

Table 1. Shadowgraph Tests Conducted

Rotor	No. of blades	Rotor radius (m)	Test configuration
Model 300 Tail Rotor	2	0.650	Hover
Sikorsky S-76	4	1.067	Hover, wake traveling down
Sikorsky S-76	4	1.067	Hover, wake traveling up
Model Tilt Rotor	3	0.610	Hover, tilt rotor
Lynx Tail Rotor	4	1.105	Hover, in ground effect
Boeing Model 360	4	1.540	Forward flight
Model Helicopter Rotor	4	0.826	Forward flight, with fuselage

Table 2. Shadowgraph Rotor Parameters

Rotor	Radius (m)	Chord (m)	Blades	Twist	Solidity	Planform
Model 300 Tail Rotor	0.650	0.120	2	0°	0.118	Rectangular
Sikorsky S-76	1.067	0.063	4	–10°	0.075	Rectangular
Model Tilt Rotor	0.610	0.057*	3	–45°**	0.089	Tapered
Lynx Tail Rotor	1.105	0.180	4	0°	0.208	Rectangular
Boeing Model 360	1.540	0.134*	4	–12°	0.101	Tapered tip
Model Helicopter Rotor	0.826	0.064	4	–12°	0.098	Rectangular

* Base chord for tapered blade

**Nonlinear twist

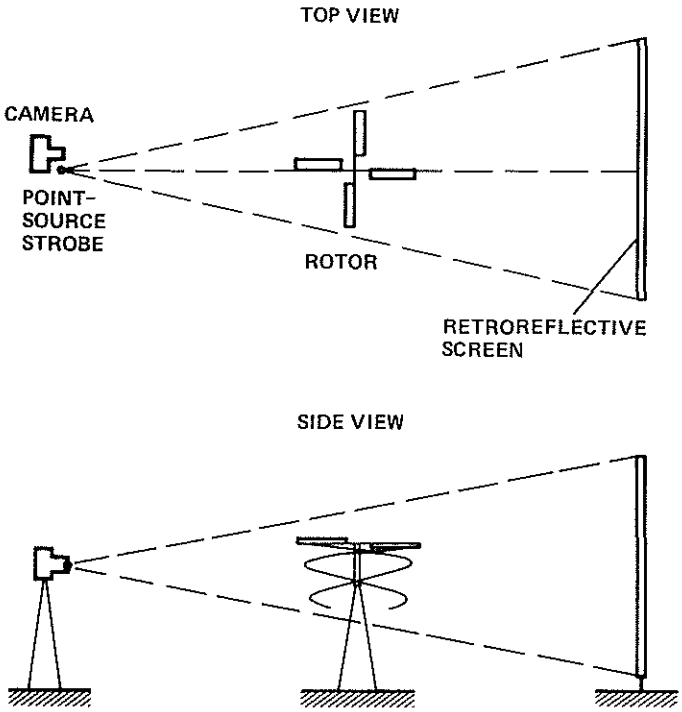


Figure 1. Shadowgraph setup.

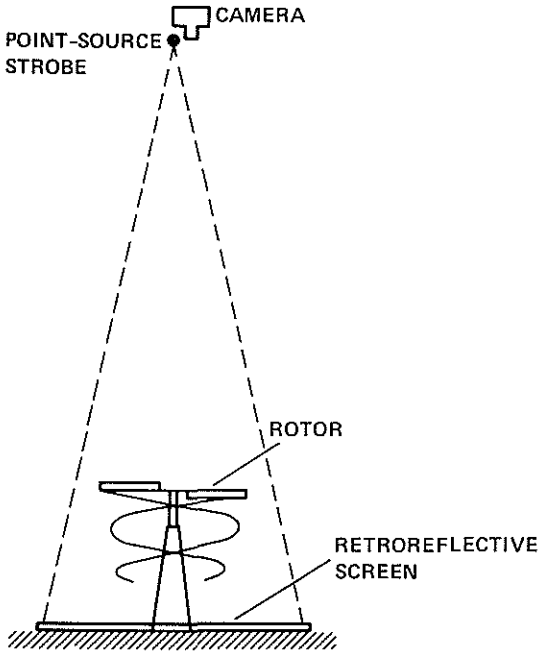


Figure 2. Alternate shadowgraph setup.

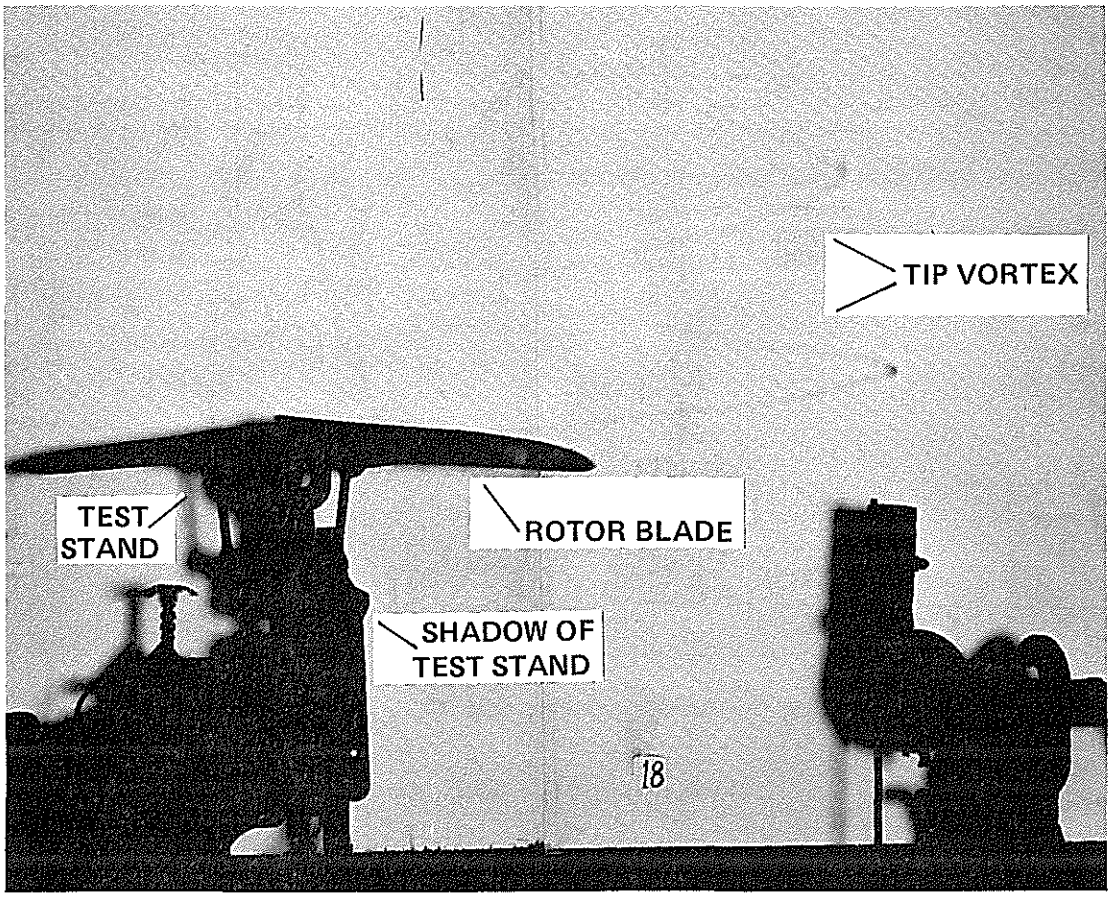


Figure 3. Shadowgraph of Hughes Model 300 Tail Rotor, $M_t = 0.38$, collective = 14°.

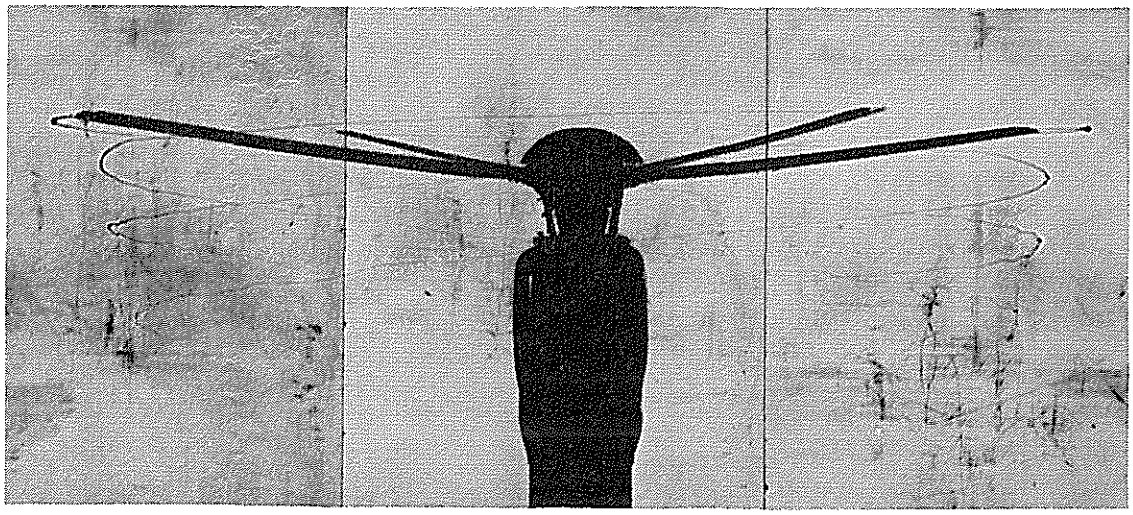


Figure 4. Shadowgraph of S-76 rotor, wake down, $C_T/\sigma = 0.103$, $M_t = 0.55$.

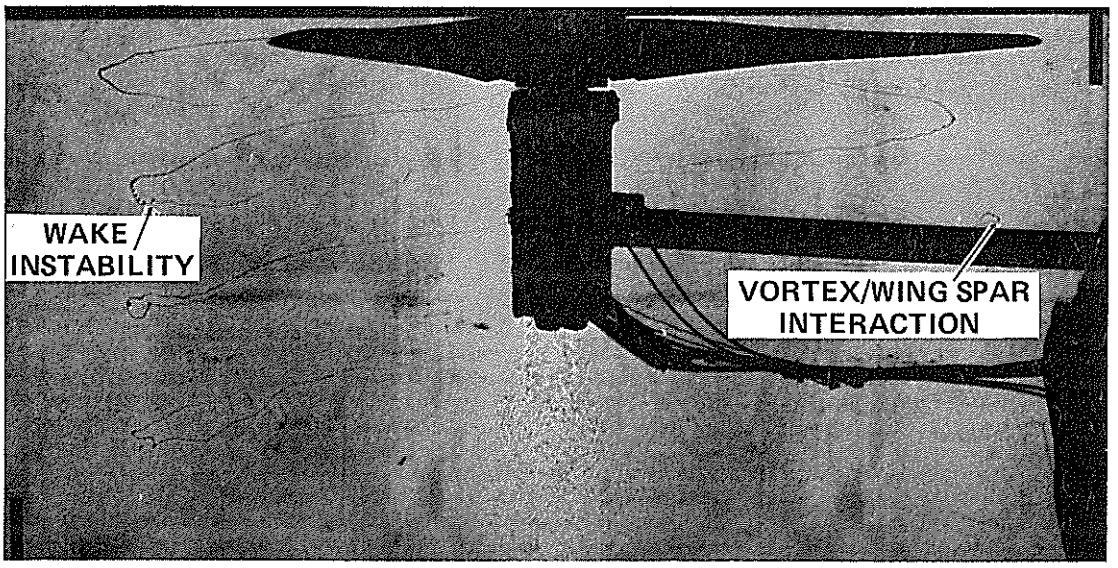


Figure 5. Shadowgraph of model tilt rotor, $C_T/\sigma = 0.083$, $M_t = 0.56$.

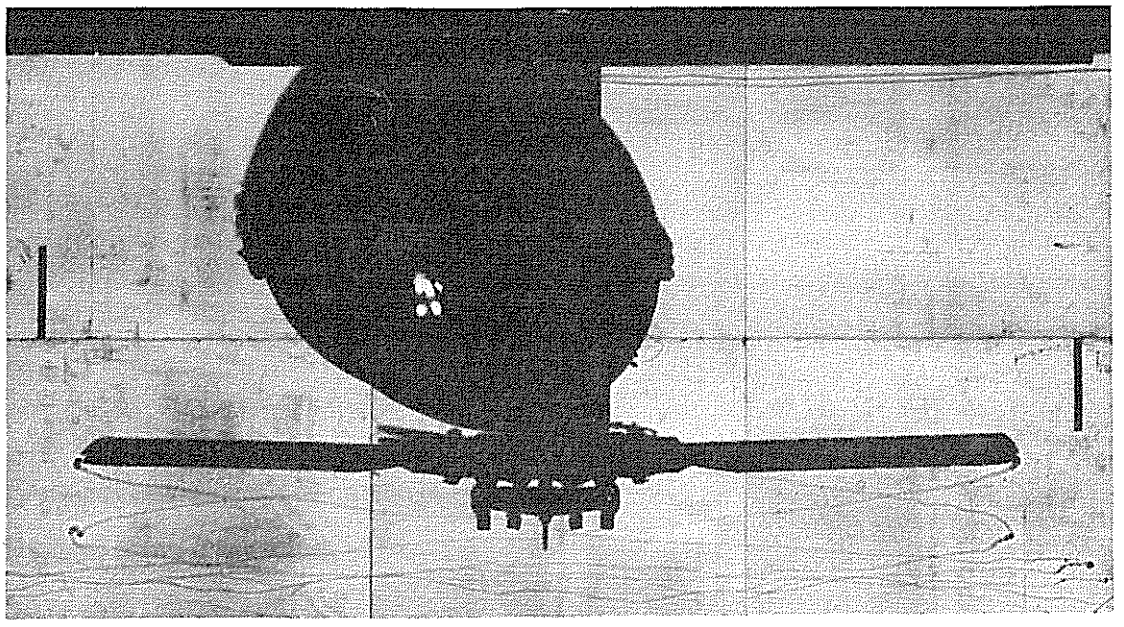


Figure 6. Shadowgraph of Lynx tail rotor in ground effect, $C_T/\sigma = 0.095$, $h/R = 0.32$.

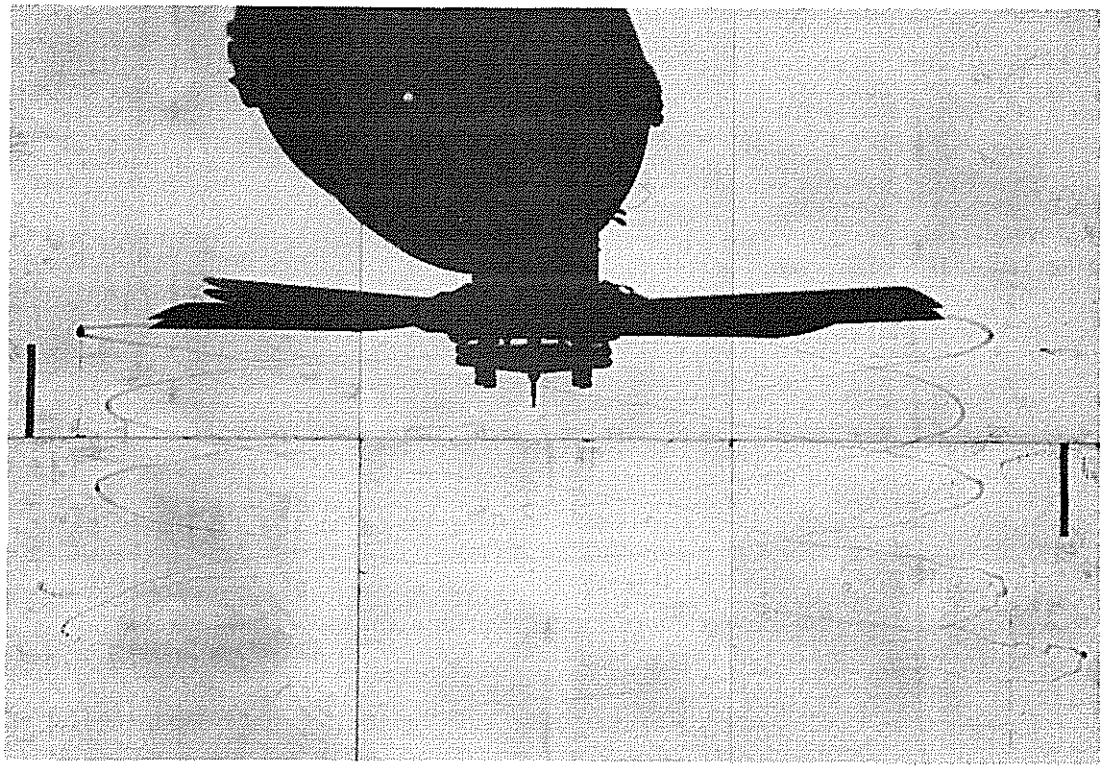


Figure 7. Shadowgraph of Lynx tail rotor in ground effect, $C_T/\sigma = 0.084$, $h/R = 0.96$.

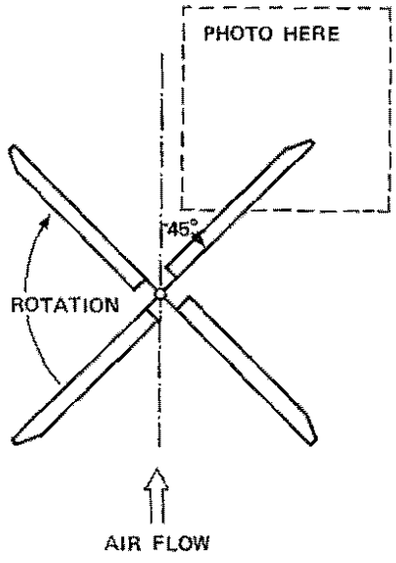


Figure 8. Schematic showing shadowgraph field-of-view from floor-mounted camera for Model 360 rotor in forward flight.

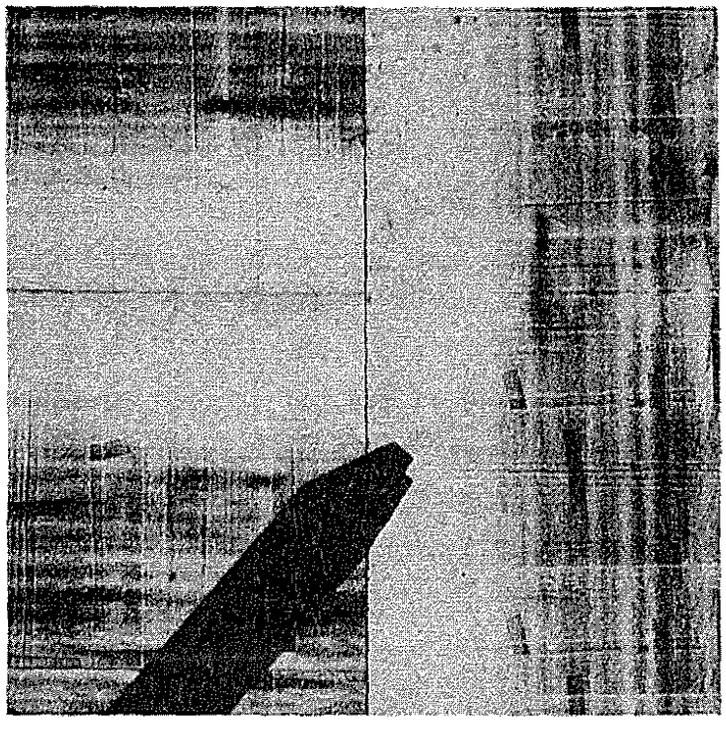


Figure 9. Shadowgraph of Model 360 rotor in forward flight, $C_T/\sigma = 0.080$, $M_t = 0.637$, $\mu = 0.069$.

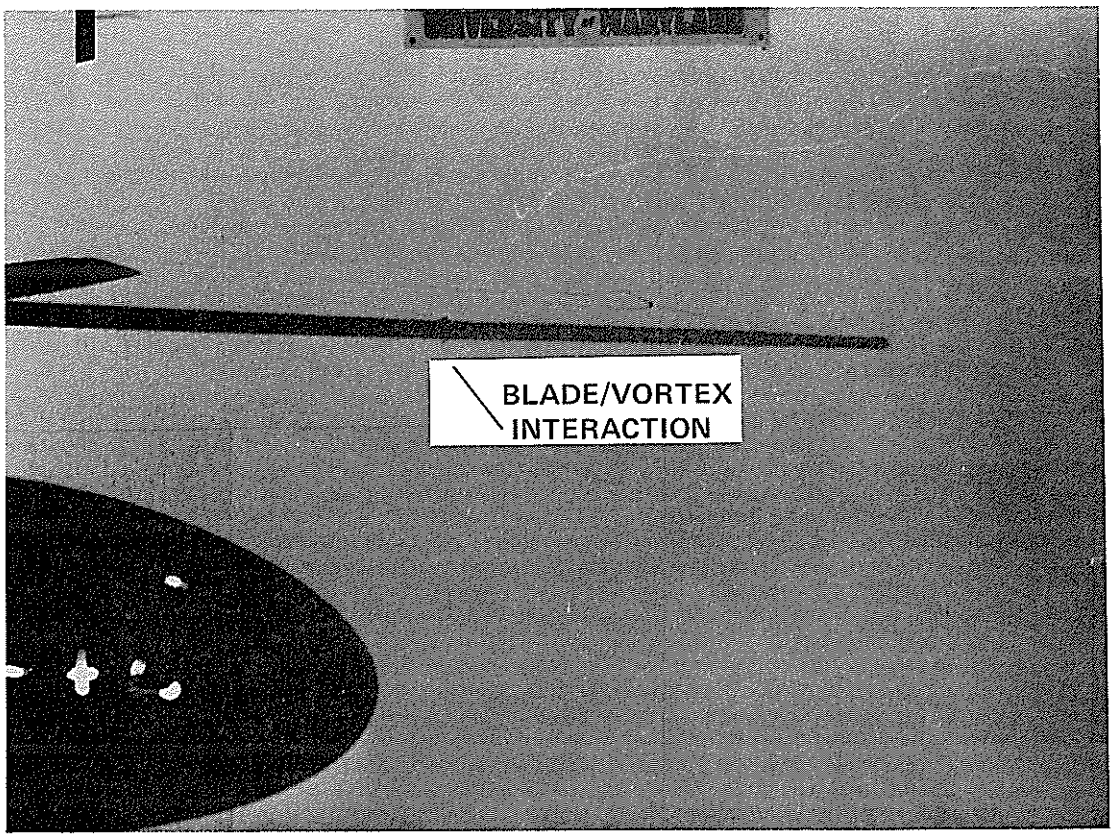


Figure 10. Shadowgraph of model rotor in forward flight, $C_T/\sigma = 0.09$, $M_t = 0.47$, $\mu = 0.05$.

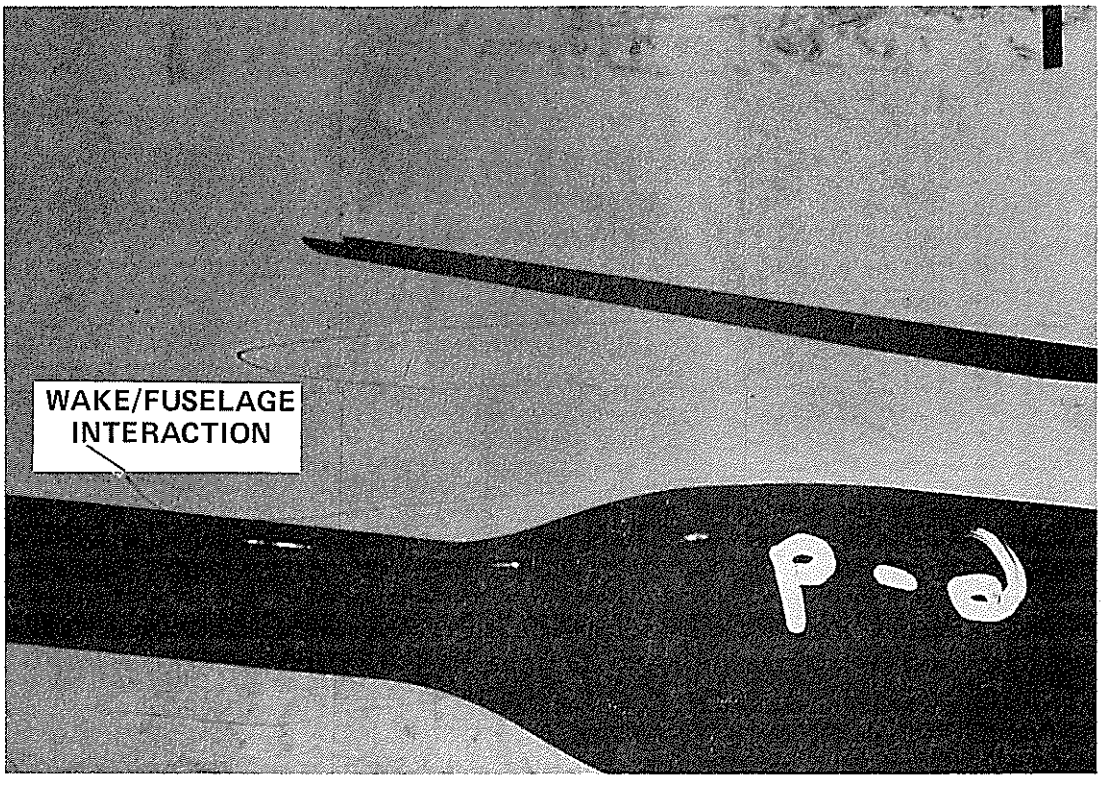


Figure 11. Shadowgraph of model rotor in forward flight, $C_T/\sigma = 0.09$, $M_t = 0.47$, $\mu = 0.05$.

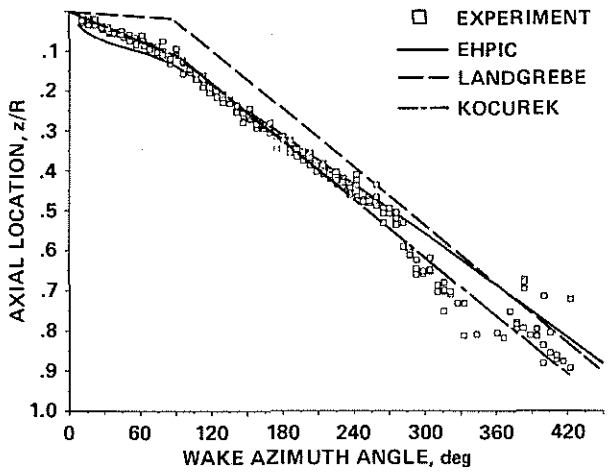


Figure 12. Comparison of measured and predicted tip vortex axial location out of ground effect, $C_T/\sigma = 0.091$.

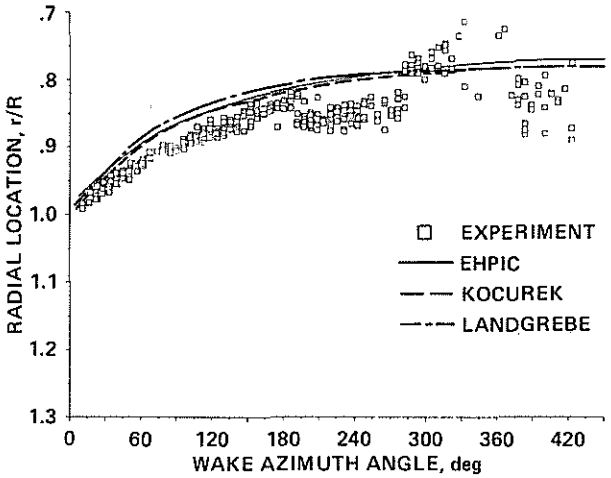


Figure 13. Comparison of measured and predicted tip vortex radial location out of ground effect, $C_T/\sigma = 0.091$.

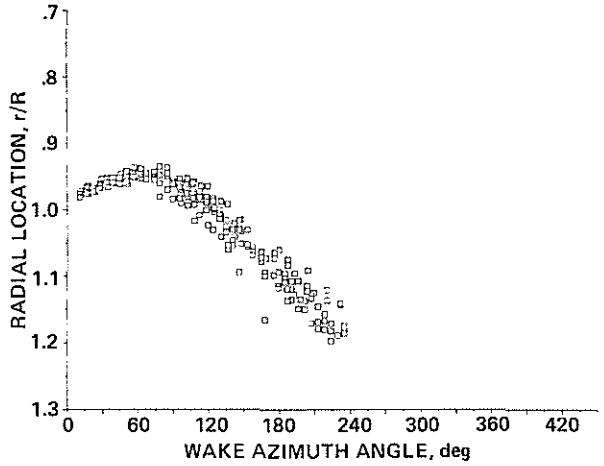


Figure 14. Radial location of tip vortex in ground effect, $C_T/\sigma = 0.095$, h/R = 0.32.

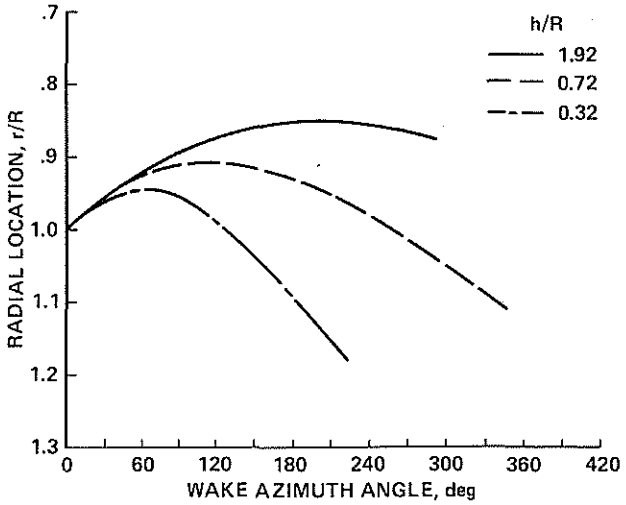


Figure 15. Effect of rotor/ground plane separation on radial tip vortex geometry, $C_T/\sigma = 0.095$.

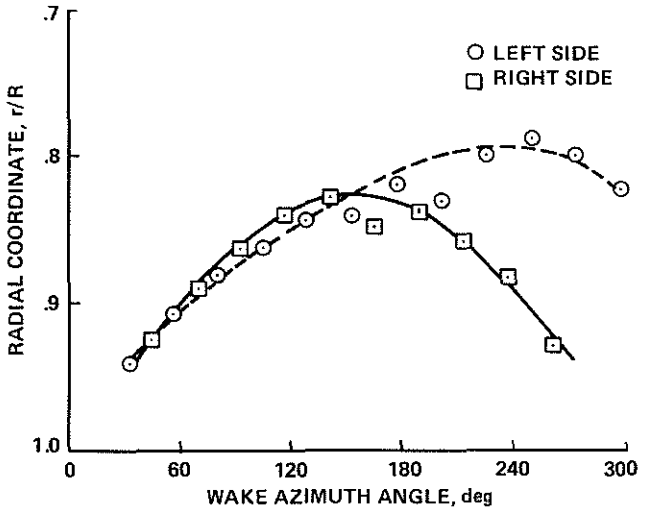


Figure 16. Radial tip vortex coordinates vs. wake azimuth angle for left and right sides of model tilt rotor, $C_T/\sigma = 0.083$, $M_t = 0.56$.